

# Singlet-triplet excitation ratios in Ne III, Ar III and N II under ion impact

E. Träbert<sup>1,2,a</sup>, H.-P. Garnir<sup>1</sup>, P.-D. Dumont<sup>1</sup>, and T. Bastin<sup>1</sup>

<sup>1</sup> Institut de Physique Nucléaire, Atomique et de Spectroscopie, Université de Liège, Sart Tilman B 15, 4000 Liège, Belgium

<sup>2</sup> Experimental physik III/NB3, Ruhr-Universität Bochum, 44780 Bochum, Germany

Received 17 November 2000 and Received in final form 31 January 2001

**Abstract.** Peculiar properties of ion-atom collision systems, in particular deviations from statistical populations of singlet and triplet levels, can be studied by optical spectroscopy. We have extended earlier studies by VUV spectroscopy of a number of collision systems at various collision energies in the 0.01-MeV/nucleon to 1-MeV/nucleon range, involving  $H_2^+$ ,  $H^+$ ,  $He^+$ ,  $He^{2+}$ ,  $Ne^+$ ,  $Ar^+$ , and  $N_2^+$  as projectiles and Ne, Ar, and  $N_2$  as target gases. Statistically significant deviations of the relative intensities of singlet and triplet lines from simple ratios are observed in the displaced terms of the valence shell of Ne III, corroborating and extending earlier work. For Ar III, the energy dependences of singlet-to-triplet excitation ratios are very different for different projectiles. For N II, in contrast, all observed line ratios are practically independent of the projectile energy.

**PACS.** 34.50.Fa Electronic excitation and ionization of atoms (including beam-foil excitation and ionization) – 34.10.+x General theories and models of atomic and molecular collisions and interactions (including statistical theories, transition state, stochastic and trajectory models, etc.) – 32.30.Jc Visible and ultraviolet spectra

## 1 Introduction

In many collision experiments that involve swift ions it is assumed that the spins of the collision partners do not change during the collision (this is often called the Wigner spin rule [1,2]). At the same time, atomic level populations after collisions are found to depend on the collision energy and to vary with the level energies and angular momenta of the final states, with no simple rules to describe the situation fully. If the population is spin-independent, levels of similar angular momentum and (almost) similar excitation energy ought to show a population proportional to the statistical weight factor  $g = 2J + 1$ , with the total angular momentum quantum number  $J$ . This would imply that the population ratio of comparable singlet and triplet levels ( $S/T$  ratio) is independent of the collision energy. Occasionally spectra are observed that seem to violate this rule, and the question arises whether a specific coupling effect is acting during the collision. The special case of neutral helium (He I) excited by ion impact, and the role of multiplet mixing of higher-lying intermediate levels reached during the collision process, have been discussed by Aynacioglu and von Oppen [3]. Beyer *et al.* [4] have studied double ionization processes in Ne with He and Ne as targets, for energies between 40 keV and 1 MeV.

They report on unresolved issues concerning the  $S/T$  ratio in comparison with work by, for example, Bloemen *et al.* [5] and by Bøving and Sørensen [6]. Most of the latter work was performed at a projectile energy of 100 keV, and the effects described were found to be much more prominent at this energy (lower than our equipment permits us to go) than near 1 MeV (the middle of our working range). An observation of possible dependencies of the  $S/T$  ratio on the projectile energy would certainly help to illuminate the collision physics involved. It seems clear, however, that the transient molecular structure of projectile and target atoms during the collision, with its peculiar symmetries and couplings often described in a molecular orbital (MO) picture [7–9], plays an important role. The physical access to the problem is difficult, because many parameters are involved. For example, the work by Bøving and Sørensen [6] used a fixed projectile energy and revealed a strong oscillatory behavior with the target atomic number. From a physics viewpoint it might be interesting to study similar processes at a given collision velocity (given collision energy in the center-of-mass system), too, as well as at various collision energies for a given collision system, and lastly collision systems with different atomic structures of the collision partners.

We therefore undertook to study a number of simple collision systems with atomic and molecular targets that permit observation with sufficient spectral resolution.

<sup>a</sup> e-mail: traebert@ep3.ruhr-uni-bochum.de

We observed ions so that the system studied would be less susceptible to external influences like stray fields, and added target species not studied previously in this way. Observation of a gas target furthermore largely removes the atomic-lifetime-ion-velocity systematic errors that plague the measurement of relative line intensities on fast projectiles in beam-foil spectroscopy. A problem not treated here is the possible collisional alignment (specific population of magnetic sublevels, see, for example, [11]) and subsequent non-isotropic light emission, since both of our detection systems were arranged for observation at right angles to the ion beam and not at the “magic angle” at which observation is insensitive to such alignment effects and to the polarization properties of the detection system [12]. However, in order to prevent a plethora of systematic errors from playing a role, we resorted to measuring line intensity ratios only and to study their possible variation as a function of projectile species and energy. This procedure avoids the problem of absolute signal normalization, in relation to target gas pressure and projectile current. Of course, such a short-cut reduces the amount of information that can be extracted from the data. Considering the complexity of the physical situation and the vagaries of detail work discussed previously (for example, Beyer *et al.* [4] state that an accurate measurement of the  $S/T$  ratio for producing  $\text{Ne}^{2+}$  in the  $^1\text{P}$  or  $^3\text{P}$  states of the  $2s2p^5$  configuration is lacking, and ascribe an uncertainty of  $\pm 100\%$  to some of their own data, which reflects the problems of any reliable calibration of the quantum efficiency of a detection system), even such a simplified approach can generate independent evidence and useful cross-checks. However, in contrast to Beyer *et al.* [4] we do not disentangle projectile and target light emission, as our spectra are dominated by the latter.

## 2 Experiment

Experiments were done at Bochum and at Liège. The Bochum experiments employed a 4 MV Dynamitron tandem accelerator delivering ions to a differentially-pumped gas target [13]. The gas target mainly consisted of a 4 cm long, 1 mm radius tube with a central gas feed. From the middle, a 2 cm long tube pointed sideways toward a 2.2 m grazing-incidence spectrometer that was equipped with a 300 l/mm concave diffraction grating and a photoelectric (channeltron) detector. After passing through the gas target, the ion beam reached a suppressed Faraday cup; the light signal was then normalized to the collected ion beam charge. The efficiency curve of the spectrometer has been determined by various methods [14–16]; it has a maximum near 20 nm and falls off smoothly towards longer wavelengths. In the wavelength range of the Ne III lines that are of primary interest here (26.7 nm to 49 nm), the relative efficiency drops almost linearly from about 0.70 to about 0.32.

The projectiles used were  $\text{H}^+$  at 0.5 MeV,  $\text{He}^+$  at 2 MeV,  $\text{He}^{2+}$  at 2 MeV and 4 MeV, all impinging on a Ne target. The spectral line widths in the measurements were 0.09 nm and 0.12 nm, achieved with spectrometer slits of

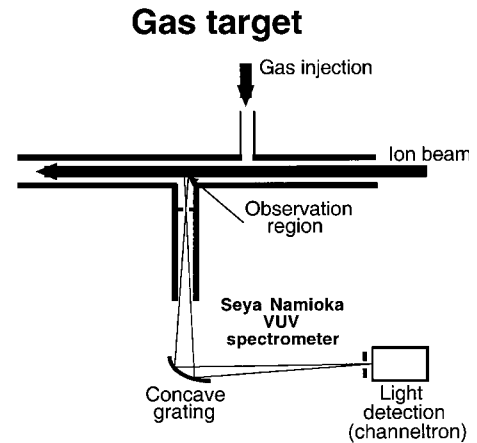
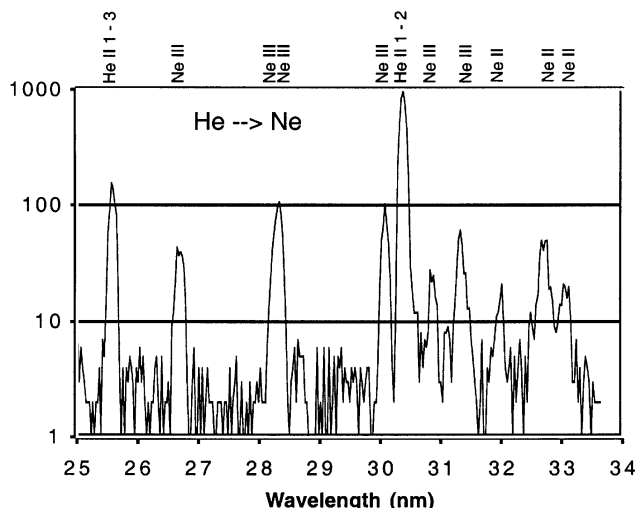


Fig. 1. Schematics of the Liège experiment lay-out.

60  $\mu\text{m}$  and 80  $\mu\text{m}$  width, respectively. The gas target was mounted in place of a foil holder on a movable and rotatable target wheel so that it could be positioned on the line-of-sight of the detection system. Gas was being fed to the target via a plastic tube of inner diameter 3 mm. The pressure of the gas supply was measured outside of the target chamber at the inlet to the plastic tube; the pressure in the center of the gas target was estimated from the pressure in the target chamber ( $10^{-6}$  mbar without gas load,  $10^{-5}$  mbar with maximum gas load), the target geometry (molecular flow), and the pumping speed of the high vacuum pumping system ( $400 \text{ l s}^{-1}$  turbo pump), to be near, but below,  $10 \mu\text{bar}$ . As expected for single-collision conditions, the ion beam current as measured on a shielded Faraday cup did not noticeably change with the admission of gas to the target; the geometric transmission through the target was 60 to 80%, depending on the ion beam focusing of the day. At the gas pressures used, no self-absorption of spectral lines of ions is to be expected.

The Liège experiments (Fig. 1) employed a 2 MV single-stage van de Graaff accelerator, an experiment chamber with a differentially-pumped gas target of 5 mm  $\times$  2 mm rectangular cross-section and 11 cm total length, a  $R = 1$  m Seya-Namioka spectrometer equipped with a 1200 l/mm diffraction grating, and a channeltron detector as used in earlier experiments [17]. The entrance slit of the spectrometer was incorporated into the gas target, so that the spectrometer-side differential pumping tube was actually inside the Rowland circle of the spectrometer. The geometrical conditions and the vacuum system were comparable to the Bochum set-up, so that the same gas pressure estimate applied to the Liège system. The whole experimental chamber was insulated and acted as a Faraday cup for the normalization of the photon signal to the integrated ion beam current. The efficiency curve of this spectrometer is not known in detail; however, the overall appearance of spectra of various elements here and when observed with spectrometers of measured efficiency curves elsewhere suggests that the efficiency is near maximum in the wavelength range near 80 nm, and that is low near 40 nm and below; however, the strong resonance line in He II (near 30.4 nm) has nevertheless been seen.



**Fig. 2.** Bochum observation of Ne III  $2p^3 3s$  level decays in the Ne gas target interspersed with He II  $1s-2p$ ,  $3p$  projectile lines. The marked Ne III multiplets and their wavelengths [18] are  $2s^2 2p^4 \ ^3P_J - 2s^2 2p^3 3s \ ^3P_{J'}$  (26.707–26.771 nm),  $^1D_2 - ^1P_1^0$  (28.249 nm),  $^3P_J - ^3D_{J'}$  (28.315–28.387 nm),  $^1D_2 - ^1D_2^0$  (30.112 nm),  $^1S_0 - ^1P_1^0$  (30.856 nm),  $^3P_J - ^3S_1^0$  (31.305–31.392 nm).

The Liège accelerator is equipped with a radiofrequency ion source that delivers only singly charged ions. This source was used to produce beams of  $H^+$ ,  $H_2^+$ ,  $He^+$ ,  $N_2^+$ ,  $Ne^+$ , and  $Ar^+$  ions and to send them into targets of Ne, Ar and  $N_2$ . Typical ion beam energies were 500 keV, 1 MeV and 1.5 MeV for most ions, but hydrogen molecular ion ( $H_2^+$ ) projectile measurements reached down to 300 keV.

### 3 Results and comparison with other data

The experiments gave rise to a number of results, ordered in the following by target species (Ne, Ar,  $N_2$ ). The spectral range of the Bochum spectrometer set-up permitted the study of levels in the  $n = 2$  (displaced terms) and  $n = 3$  shells of Ne III, while for the other target elements mostly displaced terms in the lowest electron shell ( $n = 2$  for Ne III and N II,  $n = 3$  for Ar III) were studied.

#### 3.1 Observations on the $2p^3 3s$ shell decays of Ne III (at Bochum)

The lines of the  $2s^2 2p^4 - 2s^2 2p^3 3s$  transition multiplet in Ne III lie near the  $n = 1-2$  resonance line in  $He^+$  (30.3783 nm) and are sufficiently well resolved from this and from some Ne II lines (Fig. 2). The signal rate was lowest with protons ( $H^+$ ), highest when using  $He^{2+}$  projectiles, and intermediate with  $He^+$ . Unfortunately, the recording conditions did not yield individual spectra of a statistical significance that would permit to study any detailed dependence of the relative line intensities on projectile species or energy. However, the spectra cover all singlet

and triplet terms of the  $2s^2 2p^3 3s$  configuration and their decays. This configuration gives rise to  $^1P^0$ ,  $^1D^0$ ,  $^3S^0$ ,  $^3P^0$ , and  $^3D^0$  terms.

It might be interesting to establish all individual level populations in these terms and to compare their distribution with a statistical model. However, this would be over-stressing the statistical significance of the present data. We therefore grouped the terms and summed up all singlet and all triplet level populations – and found statistical proportions there. A sum of all spectra (with the different projectiles) showed a  $S/T$  (singlet/triplet) line ratio of 1:1.8 (5% statistical uncertainty; 15% efficiency calibration uncertainty). The ratio of the sums of the statistical weight factors of the upper levels in this case is 11:18, which is close to the observed  $S/T$  intensity ratio. Cascade repopulation from higher levels is possible, but apparently this does not lead to a notable deviation from statistical ratios.

#### 3.2 Observations on the $2s2p^5$ shell decays of Ne III (at Bochum and Liège)

The ground state configuration  $2s^2 2p^4$  of Ne III gives rise to the terms  $^3P$ ,  $^1S$  and  $^1D$ . In the same  $n = 2$  shell there are displaced terms  $2s2p^5 \ ^3P^0$  and  $^1P^0$ . As there are no other decay branches, an integral observation of the transition multiplets ( $2s^2 2p^4 \ ^3P_J - 2s2p^5 \ ^3P_{J'}$  at 48.810–49.105 nm,  $2s^2 2p^4 \ ^1S_0 - 2s2p^5 \ ^1P_1^0$  at 42.784 nm, and  $2s^2 2p^4 \ ^1D_2 - 2s2p^5 \ ^1P_1^0$  at 37.931 nm [18]) reveals the relative populations of the upper levels. However, the branching of the decay of the  $2s2p^5 \ ^1P_1^0$  level to the levels  $2s^2 2p^4 \ ^1S_0$  and  $2s^2 2p^4 \ ^1D_2$  is very asymmetric, as has been confirmed in a previous measurement using, among others, the very same experimental set-up at Bochum (but with a different grating and another detector) [19]. The ratio of the relative intensities of lines from the same upper level must be independent of excitation conditions. The signal observed in five spectra recorded at Bochum with three different projectiles and at three projectile energies therefore was added up in order to take advantage of counting statistics. The signals were corrected for the relative detection efficiencies at the two wavelengths. The branching ratio result of  $(16.8 \pm 1.2)$  (statistical error;  $\pm 2.5$  efficiency curve) agrees best with the predictions by Baluja and Zeippen (17.6) [20] (from extensive configuration interaction calculations) and is not far from the predictions by Sinanoğlu (from his NCMET calculations) of 18.6 [21], and by Cheng *et al.* [22] of 15.2 (from a fewer-configuration, but fully-relativistic calculation). The previously reported experimental results ( $20.8 \pm 3.1$ ,  $23.9 \pm 3.6$ ) from a Giessen-Bochum collaboration [19] are in the same range.

The Liège data show a singlet/singlet line intensity ratio of order 3.5 to 4, from using a spectrometer without known efficiency curve, measured with  $H_2^+$  and  $He^+$  projectiles of 300 keV, 500 keV and 1 MeV, and with  $Ne^+$  projectiles of 500 keV, 1.0 MeV and 1.5 MeV. This result can now be turned around to show that the detection efficiency at the lower of the two singlet line wavelengths is

lower than at the other by a factor of about four with the Liège spectrometer set-up, underlining the steep decrease of the grating reflectivity towards shorter wavelengths.

For the ionization into the Ne III  $2s2p^5$   $^1P$  and  $^3P$  states, the Bochum data (combined from all projectiles and energies) show a  $S/T$  ratio of 1:1.5 ( $\pm 3\%$  statistical uncertainty;  $\pm 15\%$  efficiency calibration uncertainty). This is clearly different from the ratios of the statistical weight factors  $g$  of the upper levels of 1:3. In the same shell, there is another singlet level,  $2s^02p^6$   $^1S_0$ . This level feeds the  $2s2p^5$   $^1P_1^0$  level only and, by repopulation, would shift the statistical  $S/T$  ratio from 3:9 to 4:9 (or 1:2.25), if the “doubly” displaced term was excited as much as the “singly” displaced terms. This would be closer to our observation, but is still outside our error bars. Beyer *et al.* [4] claim that this cascade may induce a correction of the lower level population by up to 50% – which would reinstall statistical relations for the  $2s2p^5$  levels, but would leave to explain why the  $2s^02p^6$   $^1S_0$  level is so strongly excited. In an attempt to model such a high population of a doubly displaced term, Beyer *et al.* [4] empirically attribute a different effective charge ( $q = 1.4$  vs. 1.6) to  $He^+$  projectiles for the double ionization that leads to the excitation of the two terms. At the same time they determine an order-of-magnitude larger production cross-section for the lower (singly displaced) term, which seems to contradict the claimed large correction. Practical evidence as well as calculations of transition rates in such level systems show that most of the displaced terms do not experience much cascade feeding from regular levels in non-displaced terms. Thus any “external” cascades are unlikely to be important. Beyer *et al.* [4] also report an overpopulation of the triplet levels (in relation to the statistical expectation) at low impact energies and a trend towards  $S/T = 1:3$  for the energies used in the present experiment. They also discuss the results of other experiments [5,6] that are either statistically less certain or involve estimates rather than measurements of the detection efficiency curve. Our evidence (in our projectile energy range) points at a triplet population that is slightly below the statistical expectation when compared with the singlet level population.

The Liège data have been recorded without determining the efficiency curve of the spectrometer/detector combination. However, this is fully sufficient for the study of the variability of line intensity ratios as a function of projectile species and energy, and all further data relate to this particular problem.  $H^+$  ions of 500 keV and 1.5 MeV,  $H_2^+$  ions of 300 keV, 500 keV, and 1 MeV,  $He^+$  ions at the same three energies,  $N_2^+$  and  $Ne^+$  ions of 0.5 MeV, 1 MeV and 1.5 MeV were tried. For most projectiles, the  $S/S$  excitation ratio data show no clear (larger than, say, about 10%) change with projectile energy. An exception is the weaker of the singlet lines under bombardment with  $N_2^+$ . Tracking the line ratio of the two singlet transitions, one finds that under bombardment with nitrogen projectiles (at low projectile energies) the ratio appears to differ considerably from the mean ( $S/S \approx 0.23$ ) of the other-projectile data (Fig. 3a). A spectral blend with a projectile line (N II at 42.8 nm) is identified as the cause of the

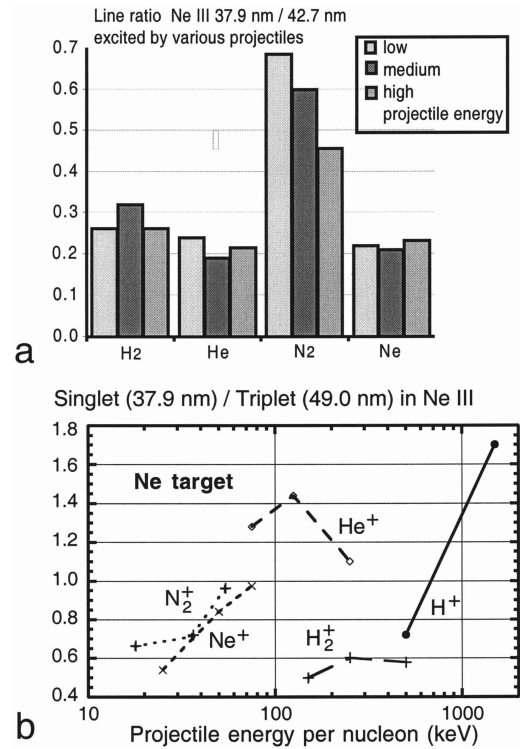


**Fig. 3.** The apparent (uncalibrated) (a)  $S/S$  and (b)  $S/T$  ratios of Ne III when excited by a variety of projectiles. Projectile energies in a) typically were 300 to 500 keV (“low”), 1 MeV (“medium”) and 1.5 MeV (“high”). In (b), the vertical scale has been adjusted by fixing the “ $H^+$  500 keV” data point to the result from averaged Bochum data on  $H^+$  and  $He^+$  at various energies (see text) in order to provide a very rough reference scale. The lines in (b) are eye-guiding only.

apparent energy-dependent deviation, and that has been taken into account by neglecting this weak decay branch for the data in Figure 3b.

With  $Ne^+$  ions impinging on Ne, the  $S/T$  ratio changes by a factor of two as a function of energy in our operating range. Beyer *et al.* [4] report a factor-of-four change over their range of study, but only for the target emission. The most striking observation is a  $S/T$  ratio with  $H^+$  and  $H_2^+$  projectiles that is lower than when using  $He^+$ , by a factor of 2.5 to 3.

This observation extends the work by Bøving and Sørensen to even lower projectile atomic numbers and confirms the finding by Beyer *et al.* [4] that for hydrogen projectiles the  $S/T$  ratio is even lower than the already low point for  $He^+$  (Bøving and Sørensen’s high points are for projectiles with half-filled outer shells, like  $B^+$  ( $Z = 5$ ),  $P^+$  ( $Z = 15$ ) and  $S^+$  ( $Z = 16$ )). If, as is also discussed by Beyer *et al.*, the promotion of two  $2s$  electrons favours the population of a  $^1P_1$  target state, while the promotion of a pair of  $2s$  and  $2p$  electrons favours statistical singlet/triplet excitation ratios, hydrogen projectiles indicate a different contribution to the excitation process again, one that disfavors the (relative) population of the singlet level.

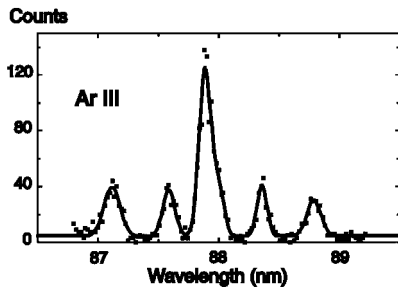


Fig. 4. Liège observation of the Ar III multiplet  $3s^23p^4\ ^3P_J-3s3p^5\ ^3P_J^0$  (87.110–88.740 nm) resolved into 5 (of 6) components. The relative intensity pattern is compatible with what is expected from a statistical population of the sublevels of the the upper term.

With  $N_2^+$  and  $Ne^+$  projectiles, the  $S/T$  ratio is about 1/3 lower than with  $He^+$ , whereas Bøving and Sørensen’s data point at slightly higher values (at their lower projectile energy). However, within about 20% error margins, all these data are compatible with each other. Thus we find the same general energy independence, but a projectile-species dependence of the  $S/T$  ratio as has been reported by Beyer *et al.* [4].

### 3.3 Observations on the $3s3p^5$ level decays of Ar III (Liège)

For Ar III, the spectroscopic situation is very comparable to that of Ne III, with spectroscopic terms of the same symmetries, except that the valence electron shell now is  $n = 3$ , and the fine structure intervals are larger. Consequently, the Ar III multiplet  $3s^23p^4\ ^3P_J-3s3p^5\ ^3P_J^0$  (87.110–88.740 nm) has been resolved into 5 (of 6) components (Fig. 4). The intensity pattern for such multiplets is known since the 1920s (apparently first systematized in [23]). The relative intensity pattern in Figure 4 is compatible with what is expected from a statistical population of the sublevels of the upper term. This observation confirms that (at least at this wavelength) our apparatus does not suffer from severe polarization effects, nor does the excitation produce a marked level of alignment – unless all of these effects combine in a way to cancel in the result.

Although the spectrum Ar III has been studied repeatedly before, the weak decay branch of the  $3s3p^5\ ^1P_1^0$  level to the  $3s^23p^4\ ^1S_0$  level has not been found, though it may be expected near 83 nm. In our spectra, two candidate lines were seen, at 82.0 nm (weaker than the stronger branch – if correctly identified – by a factor of 10) and at 82.7 nm (weaker than the line associated with the strong branch by a factor of about six). Both of these lines may still be too strong to be associated with the missing decay branch. Moreover, lower ion beam energies than ours would be needed for a sensible attempt to experimentally establish the charge states of these lines with confidence. The stronger decay branch of the same upper level, towards  $3s^23p^4\ ^1D_2$ , has been listed by Kelly and Palumbo [18] with a wavelength of 76.915 nm, but this wavelength

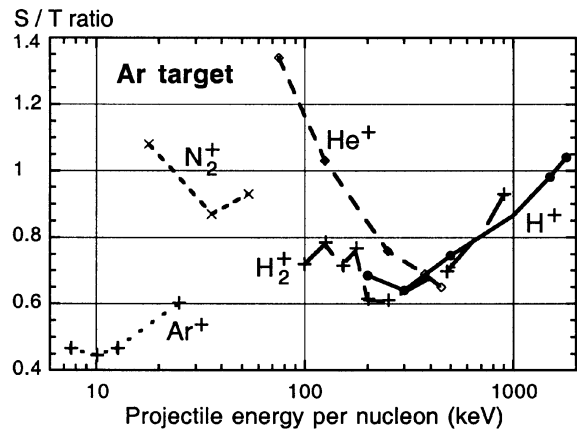


Fig. 5. Singlet-to-triplet ( $S/T$ ) excitation ratio in Ar III for various projectiles impinging on Ar. Lines between data points are for eye-guiding purpose only; the symbol sizes reflect typical statistical uncertainties.

has not been accepted for the present NIST on-line data base [24]. However, we saw a line at that position and accepted it as the one in question.

With Ar III, the complexity of the collision problem of interest becomes visually evident in Figure 5. Atomic ( $H^+$ ) and molecular ( $H_2^+$ ) ions of hydrogen were used, and apparently both yield similar effects on the  $S/T$  ratio in Ar III when comparing data at a given projectile velocity (energy per nucleon), not total energy. The  $S/T$  ratio features a minimum for a projectile energy of about 200 keV/amu, and it increases significantly towards higher projectile energies. An absolute efficiency calibration might be able to tell by the different light yields whether  $H_2^+$  acts as single, singly-charged molecule or as one or two active protons (and an electron) contributing to the excitation. With  $He^+$  projectiles, the  $S/T$  ratio is higher than with hydrogen projectiles at the lowest energies. It then decreases steeply with increasing projectile energy, in a smooth trend beyond the reduced energy at which the minimum occurs with hydrogen projectiles. In contrast to the hydrogen projectiles, no increase shows with  $He^+$  ions in the investigated range up to 450 keV/nucleon. In the range from 150 to 300 keV per nucleon, the  $S/T$  ratios are almost similar, irrespective of whether hydrogen ions, hydrogen molecular ions or helium ions cause the excitation.

With the two heavy projectiles of our selection,  $N_2^+$  and  $Ar^+$  ions, the  $S/T$  data concern a range of specific energies well below that of the hydrogen and helium data. For  $N_2^+$  projectiles the  $S/T$  ratio in our range of study remains constant (with a slight downward trend for increasing projectile energies), while with  $Ar^+$  ions, it begins at one half of the other value and then grows with increasing projectile energy. Obviously, it would be interesting to extend these latter curves towards higher energies, beyond the range of the present Liège equipment.

**Table 1.** Excitation ratios (not absolutely calibrated) in NII.

first multiplet wavelength	second multiplet wavelength	projectile		
		H <sub>2</sub> <sup>+</sup>	He <sup>+</sup>	H <sup>+</sup>
2s <sup>2</sup> 2p <sup>2</sup> <sup>3</sup> P–2s2p <sup>3</sup> <sup>3</sup> D <sup>0</sup> 108.6 nm	2s <sup>2</sup> 2p <sup>2</sup> <sup>3</sup> P–2s2p <sup>3</sup> <sup>3</sup> P <sup>0</sup> 91.7 nm	1.7	0.91	1.03
2s <sup>2</sup> 2p <sup>2</sup> <sup>3</sup> P–2s2p <sup>3</sup> <sup>3</sup> D <sup>0</sup> 108.6 nm	2s <sup>2</sup> 2p <sup>2</sup> <sup>3</sup> P–2s <sup>2</sup> 2p3s <sup>3</sup> P <sup>0</sup> 67.2 nm	1.7	1.7	11.9
2s <sup>2</sup> 2p <sup>2</sup> <sup>1</sup> D–2s2p <sup>3</sup> <sup>1</sup> P <sup>0</sup> 66.0 nm	2s <sup>2</sup> 2p <sup>2</sup> <sup>3</sup> P–2s <sup>2</sup> 2p3s <sup>3</sup> P <sup>0</sup> 67.2 nm	0.107	0.17	0.194
2s <sup>2</sup> 2p <sup>2</sup> <sup>1</sup> S–2s2p <sup>3</sup> <sup>1</sup> P <sup>0</sup> 74.5 nm	2s <sup>2</sup> 2p <sup>2</sup> <sup>3</sup> P–2s2p <sup>3</sup> <sup>3</sup> S <sup>0</sup> 64.5 nm	3.15	3.17	2.43

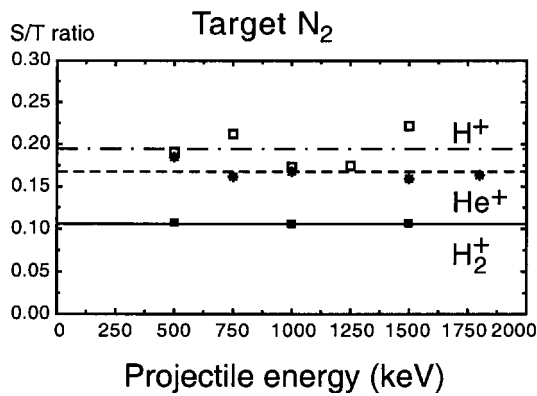


**Fig. 6.** Excitation of NII. The depicted intensity ratios of lines from the 2s2p<sup>3</sup> <sup>1</sup>P<sub>1</sub><sup>0</sup> level (66.0 nm) and from the 2s<sup>2</sup>2p3s <sup>3</sup>P<sup>0</sup> level (67.2 nm) excited by H<sup>+</sup>, He<sup>+</sup> and H<sub>2</sub><sup>+</sup> ions, respectively, are clearly different by up to a factor of two, but are not energy-dependent.

### 3.4 Observations on the 2s2p<sup>3</sup> level decays of N II (Liège)

NII was studied because it involves several notable changes compared to NeIII and ArIII. For example, in order to excite NII, a molecular target has to be broken up and excited, but only a single electron needs to be removed (or possibly one in each atomic fragment). The various 2s<sup>2</sup>2p<sup>2</sup>–2s2p<sup>3</sup> transition multiplets fall into the wide range 64 nm to 109 nm; the fine structure intervals are smaller than in Ar III and are not all resolvable with our spectrometer, and some of the lines of interest are blended with other lines. In the same wavelength range, also some 2p<sup>2</sup>–2p3s transitions (at 67.1–67.2 nm, 74.7 nm and 85.84 nm) are, in principle, accessible for measurements of S/T ratios. Our measurements did not reveal any significant variation of the line ratios in the n = 2 shell with projectile energy (Fig. 6). However, we find significantly different excitation ratios for excitation by different projectiles, that is, for H<sub>2</sub><sup>+</sup>, He<sup>+</sup>, or H<sup>+</sup>. In Table 1 we list a number of those apparent ratios (that are presumably not far from the absolute ratios, given that these are observations in the middle of our spectrometer working range).

Among the examples listed, there is a particularly notable case, involving decays of the displaced n = 2 terms 2s2p<sup>3</sup> <sup>3</sup>D<sup>0</sup> (at 108.6 nm) and <sup>3</sup>P<sup>0</sup> (at 91.7 nm) to the 2s<sup>2</sup>2p<sup>2</sup> <sup>3</sup>P ground configuration on one hand and of the 2s<sup>2</sup>2p3s <sup>3</sup>P<sup>0</sup> n = 3 term (at 67.2 nm) on the other. With H<sub>2</sub><sup>+</sup>, He<sup>+</sup>, or H<sup>+</sup> projectiles, the relative line intensity of the displaced n = 2 levels varies by no more than a factor of two. In contrast, the excitation efficiency of the 3s level drops by a full order of magnitude when using H<sup>+</sup>, the only projectile species without an electron, compared to the two other projectile species that each carry an electron. This appears to indicate the importance of the projectile electron in a process that involves not only target ionization, but also excitation.

## 4 Discussion

Our measurements concerned two target species with considerable similarities (monoatomic gases, doubly charged final ions, with terms of similar symmetries, but of n = 2 levels in NeIII and of the n = 3 levels in ArIII), and a very different molecular target (N<sub>2</sub>) in the same mass range for comparison. Considering the observed variation of the singlet-triplet excitation ratio with the projectile species, the different ionization potentials of the various projectiles spring to mind: He<sup>+</sup> (54.4 eV) has the highest, followed by Ne<sup>+</sup> (41 eV), N<sup>+</sup> (29.6 eV), Ar<sup>+</sup> (27.6 eV), and H<sup>0</sup> (13.6 eV). However, the species with almost similar ionization potentials (N<sup>+</sup> and Ar<sup>+</sup>) show clearly different population effects on the respective targets, ruling out any dominance of this parameter. (The collision system Ne + Ar was not investigated because of some expected spectral blends of target and projectile.) As H<sup>+</sup> and H<sub>2</sub><sup>+</sup> appear to yield similar results for the excitation ratios of the displaced terms studied here, the additional electron of H<sub>2</sub><sup>+</sup> (and similarly the valence electron of the neutral atom in N<sub>2</sub><sup>+</sup>) seems to be of secondary importance. In contrast, we observe a massive effect of the presence of a projectile electron on the excitation of levels in a higher electron shell in NII.

Bøving and Sørensen [6] discuss the role of single and double ionization, and they present (theoretical model) evidence for different reaction channels that are valid in

symmetric or non-symmetric collisions involving Ne as a target gas. They describe various scenarios most of which would result in a dominant population of singlet levels. Only for rare-gas projectiles they find  $S/T < 1$ . We find  $S/T$  for  $Z = 1$  (H) to be half as high as for  $Z = 10$ , an obvious underpopulation of singlet levels. The study by Beyer *et al.* [4] contains data also for  $H^+$  ions of 100 keV impinging on Ne, that is for the same energy as in the other work, with an  $S/T$  ratio that is quite compatible with ours.

All of our other projectile species are in the regions of projectile atomic number for which Bøving and Sørensen in their fixed-projectile energy experiment find relatively small deviations from statistical level population. Although the signal level in all collision systems varies strongly with the projectile energy, the  $S/T$  ratio apparently varies much less. For Ne targets, we find a marked energy dependence of the  $S/T$  ratio only for  $H^+$  projectiles. With Ar targets, observing Ar III, we have remarkably different energy dependences for the various projectile species. N II shows no  $S/T$  variation with projectile energy when bombarded by either  $H_2^+$  or  $He^+$  projectiles, but displays a clear projectile species dependence. We have not found any quantitative predictions of these phenomena in the literature.

Other experimental data and the results of molecular orbital calculations by Fritsch and Wille [25] show agreement of some cross-section trends (for double ionization, with the  $n = 2$  configurations of present interest as the final state) as a function of impact energy, but they all disagree in absolute values. To our knowledge, no appropriate theoretical treatment of the physical problem of such complex collision systems, in this energy range close to that of industrial heavy-ion accelerators, is available. New calculations might be tried on a grander scale – enabled by the dropping cost of computer power – that include more configurations and may thus be able to approximate the experimental findings better than was possible some 20 years ago. However, the technical obstacles encountered are high in both experiment and theory, trying to deal with the rich phenomenology of such ion-atom collisions. Simplifications, like in the present study of the variability of  $S/T$  level population ratios, may provide interfaces at which to check experiment *vs.* theory before launching any attempt that aims at a complete description of many-electron ion-atom collisions.

ET gratefully acknowledges support by a Belgian FNRS research grant and the cordial hospitality experienced at IPNAS. The excellent Bochum accelerator team of K. Brand and his

operators once again expanded the performance envelope of the Dynamitron tandem far beyond the design parameters – including the very low beam energies used here.

## References

1. E. Wigner, Nach. Akad. Wiss. Göttingen, 375 (1927).
2. H.S.W. Massey, E.H.S. Burhop, H.B. Gilbody, *Electronic and Ionic Impact Phenomena*, 2nd edn. (Clarendon Press, Oxford 1971), Vol. III, p. 1756.
3. A.S. Aynacioglu, G.v. Oppen, in *Fundamental Processes in Atomic Collision Physics*, edited by H. Kleinpoppen, J.S. Briggs, H.O. Lutz (Plenum Press, New York 1985), p. 745.
4. H.F. Beyer, R. Hippler, K.-H. Schartner, Z. Phys. **292**, 353 (1979).
5. E. Bloemen, H. Winter, F.J. de Heer, R. Fortner, A. Salop, J. Phys. B **11**, 4207 (1978).
6. E.G. Bøving, G. Sørensen, Phys. Rev. Lett. **40**, 315 (1978).
7. U. Fano, W. Lichten, Phys. Rev. Lett. **14**, 627 (1965).
8. M. Barat, W. Lichten, Phys. Rev. A **6**, 211 (1972).
9. J. Eichler, U. Wille, B. Fastrup, K. Taulbjerg, Phys. Rev. A **14**, 707 (1975).
10. H.F. Beyer, R. Mann, in *Progress in atomic spectroscopy*, edited by H.J. Beyer, H. Kleinpoppen (Plenum, New York 1984), p. 397.
11. T.J. Gay, H.G. Berry, R. DeSerio, H.P. Garnir, R.M. Schectman, N. Schaffel, R.D. Hight, D. Burns, Phys. Rev. A **23**, 1745 (1981).
12. R. Hippler, K.-H. Schartner, J. Phys. B **7**, 618 (1974).
13. R. Bruch, L.J. Dubé, E. Träbert, P.H. Heckmann, B. Raith, K. Brand, J. Phys. B **15**, L857 (1982).
14. E. Träbert, P.H. Heckmann, B. Raith, U. Sander, Phys. Scripta **22**, 363 (1980).
15. E. Träbert, Phys. Scripta T **8**, 112 (1984).
16. R. Jaensch, Diploma thesis, Experimentalphysik III, Ruhr-Universität Bochum, 1995 (unpublished).
17. H.-P. Garnir, T. Bastin, P.-D. Dumont, Phys. Scripta T **65**, 36 (1996).
18. R.L. Kelly, L.J. Palumbo, *Atomic and Ionic Emission lines Below 2000 Angstroms, Hydrogen through Krypton* (NRL, Washington, 1973).
19. H.-J. Flaig, K.-H. Schartner, E. Träbert, P.H. Heckmann, Phys. Scripta **31**, 255 (1985).
20. K.L. Baluja, C.J. Zeippen, J. Phys. B: At. Mol. Opt. Phys. **21**, 15 (1988).
21. O. Sinanoğlu, Nucl. Instrum. Meth. **110**, 193 (1973).
22. K.T. Cheng, Y.-K. Kim, J.P. Desclaux, At. Data Nucl. Data Tables **24**, 111 (1979).
23. H.E. White, A.Y. Eliason, Phys. Rev. **44**, 753 (1933).
24. J.R. Fuhr, W.C. Martin, A. Musgrove, J. Sugar, W.L. Wiese, NIST Atomic Spectroscopic Database, at <http://physics.nist.gov/PhysRefData/contents.html>
25. W. Fritsch, U. Wille, J. Phys. B **11**, 4019 (1978).